

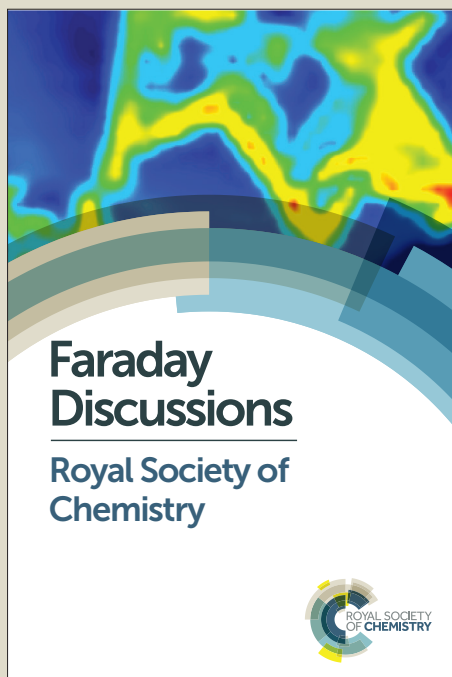
Faraday Discussions

Accepted Manuscript



This manuscript will be presented and discussed at a forthcoming Faraday Discussion meeting. All delegates can contribute to the discussion which will be included in the final volume.

Register now to attend! Full details of all upcoming meetings: <http://rsc.li/fd-upcoming-meetings>



This is an *Accepted Manuscript*, which has been through the Royal Society of Chemistry peer review process and has been accepted for publication.

Accepted Manuscripts are published online shortly after acceptance, before technical editing, formatting and proof reading. Using this free service, authors can make their results available to the community, in citable form, before we publish the edited article. We will replace this *Accepted Manuscript* with the edited and formatted *Advance Article* as soon as it is available.

You can find more information about *Accepted Manuscripts* in the [Information for Authors](#).

Please note that technical editing may introduce minor changes to the text and/or graphics, which may alter content. The journal's standard [Terms & Conditions](#) and the [Ethical guidelines](#) still apply. In no event shall the Royal Society of Chemistry be held responsible for any errors or omissions in this *Accepted Manuscript* or any consequences arising from the use of any information it contains.

This article can be cited before page numbers have been issued, to do this please use: P. Brueggeller, C. Strabler, S. Sinn, R. Pehn, J. Pann, J. Dutzler, W. Viertl, J. Prock, K. Ehrmann, A. Weninger, H. Kopacka and L. De Cola, *Faraday Discuss.*, 2016, DOI: 10.1039/C6FD00210B.



View Article Online

DOI: 10.1039/C6FD00210B

Journal Name

ARTICLE

Stabilisation effects of phosphane ligands in the homogeneous approach of sunlight induced hydrogen production

C. M. Strabler^{a,b}, S. Sinn^b, R. Pehn^a, J. Pann^a, J. Dutzler^a, W. Viertel^a, J. Prock^a, K. Ehrmann^a, A. Weninger^a, H. Kopacka^a, L. De Cola^{*a,b} and P. Brüggeller^{*a}

Received 00th January 20xx,
Accepted 00th January 20xx

DOI: 10.1039/x0xx00000x

www.rsc.org/

Most of the systems for photochemical hydrogen production are not stable and suffer from decomposition. With bis(bidentate) tetraphosphane ligands the stability increases enormously up to more than 1000 h. This stability was achieved with a system containing osmium(II) as light harvesting antenna and palladium(II) as water reduction catalyst connected with a bis(bidentate) phosphane ligand in one molecule with the chemical formula $[\text{Os}(\text{bpy})_2(\text{dppcb})\text{Pd}(\text{dppm})](\text{PF}_6)_4$. With the help of electrochemical measurements as well as photophysical data and its single crystal X-ray structure the electron transfer between the two active metal centres (light harvesting antenna, water reduction catalyst) was analysed. The distance between the two active metal centres was determined to be 7.396(1) Å. In a noble metal free combination of a copper based photosensitiser and a cobalt diimine-dioxime complex as water reduction catalyst a further stabilisation effect by phosphane ligands is observed. With the help of triethylamine as sacrificial donor in the presence of different monophosphane ligands it was possible to produce hydrogen with a turnover number of 1176. This completely novel combination is also able to produce hydrogen in a wide pH-range from pH = 7.0 to 12.5 with the maximum at pH = 11.0. The influence of monophosphane ligands with different Tolman cone angles was investigated. Monophosphane ligands with a huge Tolman cone angle ($>160^\circ$) could not stabilise the intermediate of the cobalt based water reduction catalyst and so the turnover number is lower than with an addition of monophosphane ligands with a Tolman cone angle smaller than 160° . The role of the monophosphane ligand during sunlight-induced hydrogen production was analysed and these results were confirmed with DFT calculations. Furthermore the crystal structures of two important Co(I) intermediates, which are the catalytic active species during the catalytic pathway, were obtained. The exchange of PPh_3 with other tertiary phosphane ligands can have a major impact on the activity, depending on the coordination properties. By an exchange of monophosphane ligands with functionalised phosphane ligands (hybrid ligands) the hydrogen production raised 2.17 times.

Introduction

One of the most important challenges in the next decades is the exchange of energy production systems based on fossil fuels or nuclear power with renewable energy production systems. In this context the most challenging approach is the direct transformation of solar energy into storable fuels like methanol¹ or hydrogen.² A concept for sunlight-induced hydrogen production is artificial photosynthesis. To split water into elementary hydrogen and oxygen three different complexes are important. The first one is the photosensitiser (PS), which harvests the energy of the sunlight and transfers the

energy combined with electrons to the water reduction catalyst (WRC). The photosensitiser is regenerated by the water oxidation catalyst (WOC), which produces elementary oxygen.³ The combination of the oxidation and the reduction of water is difficult and so the two different parts are split into two independent systems, the reductive part (hydrogen production) and the oxidative part (oxygen production). For the reductive part just the water reduction catalyst, the light harvesting photosensitiser and a sacrificial donor for the regeneration are needed. The photosensitiser can either be a nanoparticle⁴ (semiconductor) or can be based on a molecular compound. Two combinations in the homogeneous approach are possible, the intermolecular (both active species are in two separate molecules) and the intramolecular (both active centres are in one molecule) approach. The bridging ligand between the two different metal centres could either be conjugated^{5–8} or not conjugated.⁹ A lot of molecular photosensitisers are based on rare and expensive metals like iridium,^{10,11} ruthenium^{12,13,14,15} and osmium.⁹ Another option are noble metal free organic based photosensitisers like Eosin^{16,17} or Rhodamin dyes,¹⁸ however they are not as stable as the metal complexes and they suffer from fast decomposition. Earth abundant photosensitisers are often zinc porphyrins¹⁹ or copper based

^a University of Innsbruck, Institute of General, Inorganic and Theoretical Chemistry, Innrain 80-82, CCB – Center of Chemistry and Biomedicine, 6020 Innsbruck, Austria. E-mail: peter.brueggeller@uibk.ac.at; Tel: +43 (0)512 507 57006

^b ISIS & icFRC, Université de Strasbourg & CNRS, 8 rue Gaspard Monge, 67000 Strasbourg, France. E-mail: decola@unistra.fr; Tel: +33 (0)3 6885 5220

Electronic Supplementary Information (ESI) available: kinetic constants, syntheses and characterisation of PS X, Co-WRC, Co(I) intermediates with PPh_3 and PMePh_2 , different hydrogen production measurements with PMe_2Ph , $\text{P}(n\text{Bu})_3$, $\text{P}(t\text{Bu})_3$, $\text{P}(2\text{-An})_3$ and $\text{P}(4\text{-An})_3$ as phosphane ligands; theoretical parameters of the calculated structures; X-ray parameters of the measured complexes; CCDC 1483181-1483182 and 1501824; See DOI: 10.1039/x0xx00000x

homoleptic $[\text{Cu}(\text{NN})_2]^+$ ²⁰ or heteroleptic $[\text{Cu}(\text{NN})(\text{PP})]^+$ ^{21–23} complexes. This Cu(I) can also be connected to surfaces like TiO_2 to increase the stability of the system.²¹ With their interesting photophysical properties they could also be applied as luminescence based sensitizers, light emitting electrochemical cells (LECs)²⁴ or organic light emitting diodes (OLEDs).²⁵ The water reduction catalysts can either be bioinspired complexes from iron^{15,26} or nickel^{14,17,27} or can be cobalt complexes,^{10,28,29} developed for electrocatalytic hydrogen production. Most of the catalytic active cobalt WRCs are made out of bidentate or

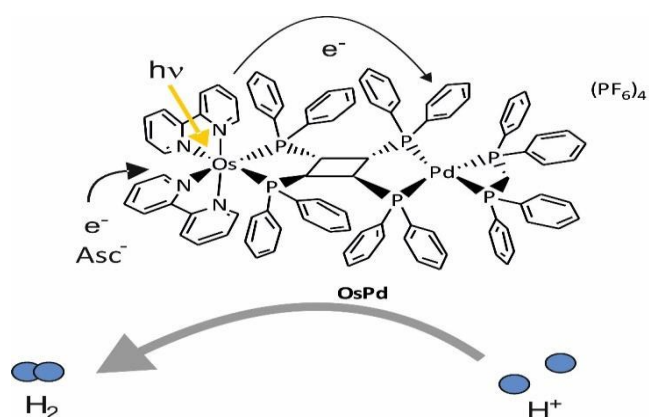


Figure 1: Osmium(II) as light harvesting antenna is excited by sunlight and transfers an electron to the palladium(II) metal centre by oxidative quenching of the chromophore. The repetition of this process and the simultaneous presence of reductive quenching reduce two protons to one elementary hydrogen; the oxidised species of osmium is regenerated by ascorbic acid

tetradentate N-ligands, which are inspired from the cobaloxime motive. In the intramolecular approach the catalytic active centre is typically based on palladium.⁹

At this point it is important to emphasize that sacrificial conditions are used in this work. However, there are at least three possibilities how it is possible to move away from this situation: the first possibility is to combine a system consisting of a PS and a WRC with a suitable WOC instead of a sacrificial electron donor. The second possibility is related to the question: is it absolutely necessary that water remains the supply of electrons in artificial photosynthesis? This means, that a sacrificial electron donor consisting of an inexpensive, environmentally benign and sustainable material could also be a solution of this problem. Possible candidates are e.g. methanol or sulphite. Also natural products where the oxidized form could be used commercially are interesting. However, in this work ascorbic acid and triethylamine have been used successfully as sacrificial donors for the intramolecular and the intermolecular systems, respectively. Ascorbic acid was not applicable for the intermolecular system at all and triethanolamine gave a considerably poorer result. The third possibility is to deliver the electrons in an electrocatalytic way. This means that peak current could be stored in high energy chemicals like hydrogen. It is well-known that especially the cobalt complexes presented in this work are also suitable for electrocatalytic applications.

Investigations in an intramolecular system

Hydrogen production

View Article Online

DOI: 10.1039/C6FD00210B

In this work, a modification of the first dppcb (*cis,trans,cis*-diphenylphosphanylchlorobutane)³⁰ based active dyad $[\text{Os}(\text{bpy})_2(\text{dppcb})\text{Pd}(\text{bpy})](\text{PF}_6)_4$ ⁹ with an exchange of bpy (2,2'-bipyridine) at the palladium side of the dyad with dpmp (diphenylphosphanylmethane) is reported. A preliminary report of the photocatalytic behaviour of $[\text{Os}(\text{bpy})_2(\text{dppcb})\text{Pd}(\text{dpmp})](\text{PF}_6)_4$ has already been given.⁹ With this modification the activity and the stability of the system increased. To investigate the energy-based electron transfer the homometallic complexes for the photosensitizer $[\text{Os}(\text{bpy})_2(\text{dppcb})\text{Os}(\text{bpy})_2](\text{PF}_6)_4$ ³¹ and $[\text{Os}(\text{bpy})_2\text{cis-dppen}](\text{PF}_6)_2$ ³² and $[\text{Pd}(\text{dpmp})(\text{dppcb})\text{Pd}(\text{dpmp})](\text{PF}_6)_4$ for the water reduction catalyst were synthesised (see ESI, page 2). With these complexes and their electrochemical and photophysical properties a photoinduced electron transfer was detected. A cartoon for this active system is illustrated in Figure 1.

With our intramolecular approach we investigate the reductive half reaction of sunlight induced water splitting. For

Table 1: hydrogen production of $[\text{Os}(\text{bpy})_2(\text{dppcb})\text{Pd}(\text{dpmp})](\text{PF}_6)_4$ with different light sources

light source	stability (h)	TON
LED 447 nm (550 mW)	> 350	37
LED 405 nm (270 mW)	> 350	40
LED cold white (550 mW)	> 350	38
Hg-lamp (700 W)	243	267
Hg-lamp (700 W) 395 nm cut off	1412	113

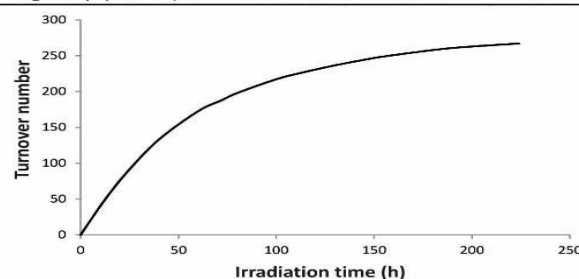


Figure 2: Time dependent hydrogen production of $[\text{Os}(\text{bpy})_2(\text{dppcb})\text{Pd}(\text{dpmp})](\text{PF}_6)_4$ (0.1 mmol/L) in a solution of $\text{ACN}:\text{H}_2\text{O}$ 4:5 (v/v, 9 mL) with an addition of 1000 eq. ascorbic acid as sacrificial donor; irradiation source = Hg-medium pressure lamp (Fe₃ doped)

the required electrons a so called sacrificial donor is needed, which reduces the photosensitizer and will be destroyed itself. To exclude the hydrogen production of elementary palladium some elementary mercury was added, because it is well known, that elementary palladium with a suitable size can also produce hydrogen in the presence of the sacrificial donor (electron donor) and a photosensitizer. The general procedure of the hydrogen measurement is explained in the supplementary information. During our measurements we determined, that elementary palladium could not produce hydrogen under our irradiation conditions. When elementary palladium was produced the activity of the system was reduced and so the destruction of our dyad. All the catalytic experiments with $[\text{Os}(\text{bpy})_2(\text{dppcb})\text{Pd}(\text{dpmp})](\text{PF}_6)_4$ were carried out in a solution

of acetonitrile and water with a ratio of 4:5 (v/v) (9 mL) and a concentration of 0.1 mmol/L of the dyad. 1000 eq. of ascorbic acid were added as sacrificial donor and the solution was freeze pump thawed two times before the addition of the compounds and two times after the addition. The produced hydrogen TON values with $[\text{Os}(\text{bpy})_2(\text{dppcb})\text{Pd}(\text{dppm})](\text{PF}_6)_4$ as dyad and ascorbic acid as sacrificial donor are illustrated in Table 1. Based on all these measurements the stability of

started at 420 nm) we obtained a very high stability of more than 350 h with turnover numbers of approximately 40. The activities of the measurements with the LEDs and with the mercury medium pressure lamp including a cut off filter at 395 nm are comparable. However, the activity with the mercury medium pressure lamp without any cut off filter is 2.4 times higher. The wavelengths with higher energy values increase the activity, because the molecule will be excited more often and the electron transfer happens occasionally. The higher energy contribution could also populate the $^3\text{MLCT}$ state of the osmium metal centre, thus leading to charge separation. In Figure 2 the time dependent hydrogen production is illustrated.

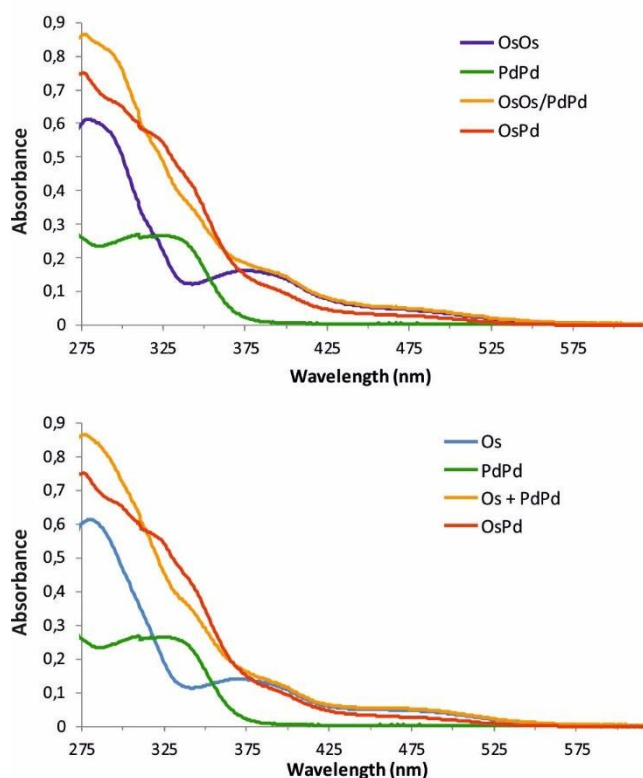


Figure 3: above: UV-Vis spectra of OsOs (dark blue line), PdPd (green line), a mixture of OsOs and PdPd (orange line) and OsPd (red line); the isoabsorptive points of OsOs and PdPd are at 322 nm and 355 nm; below: UV-Vis spectra of Os (light blue line), PdPd (green line), a mixture of Os and PdPd (orange line) and OsPd (red line); the isoabsorptive points of Os and PdPd are at 322 nm and 355 nm as well

$[\text{Os}(\text{bpy})_2(\text{dppcb})\text{Pd}(\text{dppm})](\text{PF}_6)_4$ is excellent. With the mercury medium pressure lamp and a cut off filter of 395 nm the stability of the system with 1412 h is extraordinary long. This stability is enormous, because all the other intramolecular approaches for light-induced hydrogen production just have stabilities less than 50 h.^{5-7,33} The phosphane ligands are able to stabilise the lower oxidation states of osmium (Os(I)) and of palladium (Pd(0)) and therefore the stability during the catalytic pathway increases. However, the activity with a turnover number of 113 is lower than without any cut off filter. In the very similar experiment without any cut off filter systems (only FeI_3 doped lamp), we obtained also a good stability with 243 h and a much better activity with a turnover number of 267. With different kinds of LEDs with 447 nm, 405 nm and a cold white LED (spectrum

Investigation of the electron transfer

To understand the electron and the energy transfer in an intramolecular system more clearly, it is important to do all the photophysical measurements with different homo- and heterometallic complexes. For the light harvesting part the osmium complexes $[\text{Os}(\text{bpy})_2(\text{dppcb})\text{Os}(\text{bpy})_2]^{4+}$ (OsOs)³¹ and $[\text{Os}(\text{bpy})_2(\text{cis-dppen})]^{2+}$ (Os)³² and for the reductive part $[\text{Pd}(\text{dppm})(\text{dppcb})\text{Pd}(\text{dppm})]^{4+}$ (PdPd) (see ESI, Figure 1) were measured. The monometallic $[\text{Pd}(\text{dppm})(\text{cis-dppen})]^{2+}$ is not synthesisable based on ligand exchange during synthesis. First, the UV-Vis measurements were performed to obtain the transition states of the OsPd dyad. The maxima of the absorption peaks and the ϵ of all complexes are already published.^{9,31,32} The combined UV-Vis spectrum of OsOs and PdPd (orange line in Figure 3 above) shows a different UV-Vis spectrum compared to the OsPd dyad. The MLCT state of the osmium centre is less pronounced than in the OsOs complex and the peaks of the MC state of Pd and the LC state of the bpy ligands are slightly better separated (orange and red line in Figure 3). This means that an influence of the metal centres upon each other is certain. The same result is obvious with a combination of Os as photosensitiser and PdPd as homometallic Pd complex (see Figure 3 below). All the measurements were performed with the same concentrations of the metal centres ($2.0 \cdot 10^{-5}$ mol/L for OsOs and PdPd and $4.0 \cdot 10^{-5}$ mol/L for Os and OsPd). With these UV-Vis measurements, a possible energy transfer from one metal centre to the other one can be determined. For this reason the photophysical measurements of the complexes OsOs and Os alone, OsOs with PdPd, Os with PdPd and OsPd were measured in a solution of ACN and water (1:1). This solution was chosen, because the photocatalytic measurements also were performed in a mixture of ACN and water. To characterise the photophysical properties of the osmium metal centre the complexes were excited at 405 nm. For the investigation of the energy transfer the luminescence quantum yields of all complexes were performed. The luminescence quantum yields of the homometallic complexes are quite similar with 5.7 % of Os (in DMSO 6.4 %³²), 4.5 % of *rac*-OsOs and 5.7 % of *meso*-OsOs. However, the luminescence quantum yield of OsPd of 2.2 % is significantly lower. With these measurements it is obvious that an electron transfer from the osmium to the palladium metal centre occurs. The excited state lifetime of *meso*-OsOs is with 343 ns in the same range as the

excited state lifetime of Os with 339 ns and considerable longer than of the *rac*-OsOs with 247 ns. The excited state lifetime of the OsPd is bi-exponential because two different pathways are possible. The first excited state lifetime has a value of 323 ns (50 %) in degassed ACN and is based on a classical ³MLCT mechanism of the osmium metal centre.⁹ The second one with 116 ns (50 %) is based of an electron hopping mechanism from the ¹MLCT of the osmium to the MC state of the palladium and back to the ³MLCT state, because the energy levels of the osmium ³MLCT (-3.98 eV) and the palladium MC states (-4.03 eV) are really close to each other. The kinetic constants of the complexes are discussed in the ESI, pages 2 and 3.

The HOMO and the LUMO energy levels are calculated using the electrochemical and photophysical measurements of OsPd⁹ and PdPd, where the detailed parameters of this complex are given elsewhere. The palladium metal centre has a HOMO energy level of -7.64 eV and a LUMO energy level of -4.03 eV, whereas the energy levels of the osmium are at -6.17 eV (HOMO) and -3.54 eV (LUMO). With these energy levels and with the photophysical measurements the Dexter and the Förster energy transfer can be excluded. The Förster energy transfer mechanism is not possible, because the emission of the osmium (633 nm) is not able to excite the palladium metal centre with a maximum of the absorption at 342 nm. The Dexter mechanism is also not possible, because the energy level of the HOMO-palladium is quite lower than the energy level of the HOMO-osmium and so no electron hopping is possible. The most possible energy transfer is the so called PET (photoinduced electron transfer). During this mechanism a charge separation is happening and the osmium is oxidized from Os(II) to Os(III) and the palladium is reduced from Pd(II) to Pd(I). To lose the energy the electron is transferred again to the osmium metal centre or the electron can be used for reduction reactions like hydrogen production. With these calculations and with the suitability of the OsPd dyad to produce hydrogen the PET is the most likely energy coupled electron transfer.

Crystal structure

In Figure 4 it is obvious that the cyclobutane ring system is not twisted. Due to the ancillary ligand at the palladium metal centre the cyclobutane ring system could not be twisted to avoid strain in the fused four- and five-membered rings. Another very interesting point

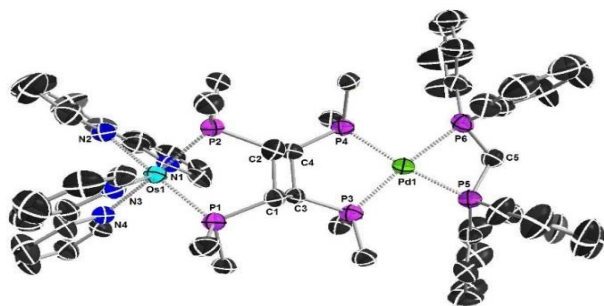


Figure 4: Crystal structure of Os(bpy)₂(dppcb)Pd(dppm)(PF₆)₄; the phenyl groups of dppcb, the counteranions, the solvent molecules and the hydrogen atoms are omitted for clarity; the most important distance of this compound is the distance between the two metal centres with 7.396(1) Å; based on the *trans*-influence the bond lengths between the phosphorus atoms and the palladium metal centre are slightly longer; the other bond lengths and angles are given in the supporting information.

in this structure is the bond length between the phosphane donor groups and palladium as metal centre, because based on the *trans* influence they are longer than usual (see ESI, page 4). The most important parameter of the crystal structure is the distance of the two metal centres (osmium and palladium) with 7.396(1) Å. This small distance between the two metal centres enables either an energy or an energy coupled electron transfer. The photoinduced electron transfer is the most common one and is discussed above. The phenyl groups of the different phosphane donor groups of the bridging ligand dppcb have a distance of more than 4 Å to each other and so no π-π stacking is possible. This is another confirmation that the energy transfer can only happen by orbital overlap of the two different metal centres (osmium and palladium).

Investigations in an intermolecular system

The first combinations of Cu(I) based photosensitisers and Co based water reduction catalysts were investigated by Castellano and co-workers.^{20b} They obtained a hydrogen production with a TON of 35 after one cycle and after few cycles with the addition of WRC they obtained a TON of 200 after 120 h. M. Fontecave and co-workers obtained a TON of 680 with the cobalt based water reduction catalyst [Co(III)(DO)(DOH)pnBr₂], which was also used in this work, however with an iridium based photosensitiser.¹⁰ By an exchange of this iridium based photosensitiser with a Cu(I) based photosensitiser we could increase the activity by simultaneous cost reduction.³⁴ A promising hydrogen production with a turnover number up to 1176 was obtained with the combination of [Co(III)(DO)(DOH)pnBr₂]⁵ as water reduction catalyst, [Cu(Xantphos)(Bathocuproine)](PF₆)^{22,23,35} as photosensitiser, with triethylamine as sacrificial donor and an addition of phosphane ligands. The influence of phosphane ligands with different properties (electronic density, Tolman cone angle) was analysed with analytic methods like CV-measurements as well as time resolved UV-Vis spectroscopy and confirmed with theoretical calculations (time resolved density functional theory). The main components of the photocatalytically active system are illustrated in Figure 5.

The hydrogen production measurements were performed in a mixture of ACN and water (v/v = 1:1, see also ESI, chapter 5)

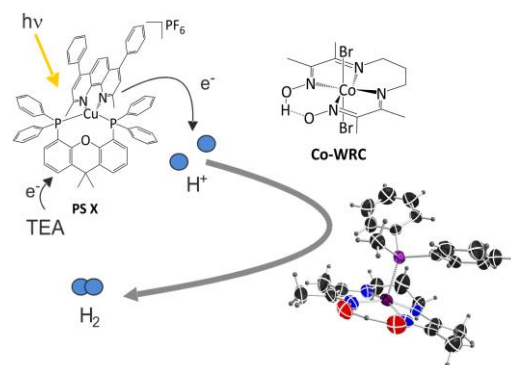


Figure 5: PS X as copper based photosensitiser is able to reduce Co-WRC as cobalt based water reduction catalyst twice, which is stabilised by an addition of phosphane ligands and the reduced Co(I) intermediate of Co-WRC reduces two protons to one molecule hydrogen; the oxidised form of PS X is regenerated by TEA as sacrificial donor.

with 10 % of the sacrificial donor. The procedure describing these photocatalytic tests is reported in the ESI, page 2. The pH-value was adjusted with hydrochloric acid. If one component (PS, WRC, TEA) was excluded no significant hydrogen production was detectable. The addition of phosphane as stabiliser of the later described active species of Co-WRC is very important, because the activity was increased from a turnover number of 392 without any addition of phosphane ligands to a turnover number of approximately 680 with an addition of phosphane ligands (PMePh₂ = 671; PMe₂Ph = 675; PPh₃ = 681) (Entries 1,2,3 and 4 in Table 2). With a higher pH-value, the hydrogen production increased (Entry 5 in Table 2). Both a higher and a lower concentration of all the components led to a decreased activity (Entries 6 and 7 in Table 2). The experiments with different ratios in relation to PS X and Co-WRC showed that the photosensitiser is more stable than the water-reduction

Table 2: Different active hydrogen production systems with PS X and Co-WRC at different ratios, different pH-values and with an addition of different phosphane ligands; a Hg-medium pressure lamp (700 W) was used as irradiation source; a = PMePh₂, b = PMe₂Ph, c = PPh₃, d = PPh₂CH₂CH₂NH₂, e = LED (405 nm) as irradiation source.

Entry	PS X [μmol/L]	Co-WRC [μmol/L]	phosphane [μmol/L]	pH	PS TON	WRC TON
1	60	90		10	392	261
2	60	90	180 ^a	10	671	448
3	60	90	180 ^b	10	675	450
4	60	90	180 ^c	10	681	454
5	60	90	180 ^a	11	738	492
6	120	180	360 ^a	10	514	343
7	30	45	90 ^a	10	548	365
8	60	60	120 ^a	10	542	542
9	120	60	120 ^a	10	270	540
10	180	60	120 ^a	10	175	525
11	60	120	240 ^a	10	942	471
12	60	180	360 ^a	10	1176	392
13	60	90	90 ^a	11	711	474
14	60	90	270 ^a	11	759	506
15	60	90	360 ^a	11	762	508
16	60	90	450 ^a	11	759	506
17 ^e	60	90	180 ^b	11	415	277
18 ^e	60	90	180 ^d	11	901	601

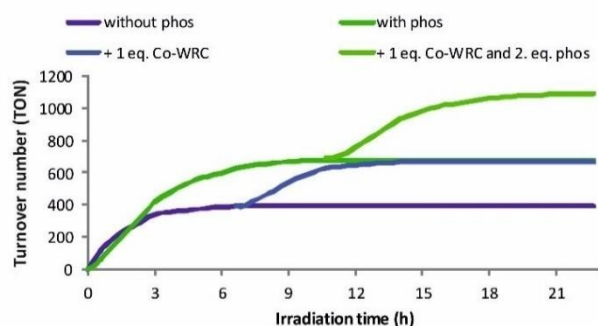


Figure 6: Time dependent hydrogen production without any phosphane ligand (dark blue) and with PPh₃ (dark green); After an addition of 1 eq. of Co-WRC the system is able to produce hydrogen again (light blue, light green); pH-values of the irradiated solutions with and without phosphane ligand = 10.

catalyst. The reaction with a ratio of 1:1 (PS X:Co-WRC) gave a TON of 542. Very similar results were obtained with a ratio of 2:1 and a ratio of 3:1 (Entries 8, 9 and 10 in Table 2). In contrast to these experiments the hydrogen production increased with a higher concentration of WRC. With ratios of 1:2 and 1:3 TONs of 942 and 1176 were obtained, respectively (Entries 11 and 12 in Table 2). Two equiv. of either PPh₃, PMePh₂ or PMe₂Ph were added to each measurement. An addition of 2 equiv. of a phosphane ligand is necessary. With just one equiv. of PMePh₂ the hydrogen production is slightly lower with a TON of 711 (pH = 11) (Entry 13). Higher concentrations of phosphane ligands did not have any influence on the hydrogen production (Entries 14, 15 and 16 in Table 2). All these solutions were irradiated with a Hg-medium pressure lamp (700 W) as light source. With a LED (405 nm, 5 W) the hydrogen production was slightly lower with a TON of 415 and so this system did not need high power irradiation sources to produce hydrogen. After an exchange of PPh₃ with a hemilabile ligand (PPh₂CH₂CH₂NH₂) the hydrogen production increased 2.17 times (Entries 17 and 18). The exchange of TEA with triethanolamine (TEOA) or ascorbic acid as sacrificial donor reduced the activity enormously. With TEOA as sacrificial donor a TON of 120 (with the conditions of Entry 3) was achieved and with ascorbic acid the system was not active (with the conditions of Entry 3), which was further proven by the formation of elementary copper.

The activity of the water reduction catalyst with the addition of phosphane ligands decreased slightly, however the stability of the system increased in the presence of phosphane ligands enormously (see Figure 6). The phosphane stabilised the Co(I)-intermediate of the catalyst, so that the catalyst could produce hydrogen twice as long as without any addition of phosphane ligands at a pH-value of 10 (with PPh₃ = 10 h (green line in Figure 6), without PPh₃ = 5.5 h (blue line)). The stability of the Cu(I) photosensitiser is higher than the stability of the catalyst. After an addition of 1.5 eq. of Co-WRC to an inactive system of PS X and Co-WRC (after an irradiation of 5.5 h) the hydrogen production started again and the production increased from a turnover number of 392 to 612 (pH-value = 10) (light blue line). The same results were obtained by the similar experiments with an addition of PPh₃. The obtained turnover number increased from 693 after 10 h to 1087 after an addition of 1 eq. of Co-WRC and 2 eq. of PPh₃ (light green line). No hydrogen production was measured after an addition of 1 eq. of PS X after 5.5 h to a newly irradiated system.

Influences of the pH-value

The right pH-value is very important for this system. In the range of 1-6.0 PS X was destroyed by a side reaction to elementary copper. The redox potential of Cu(I) to Cu(0) is positive and so the Cu(I) metal centre is reduced to elementary copper, whereas at basic conditions the redox potential of Cu(I) to Cu(0) is negative and the Cu(I) metal centre is stable. To analyse the

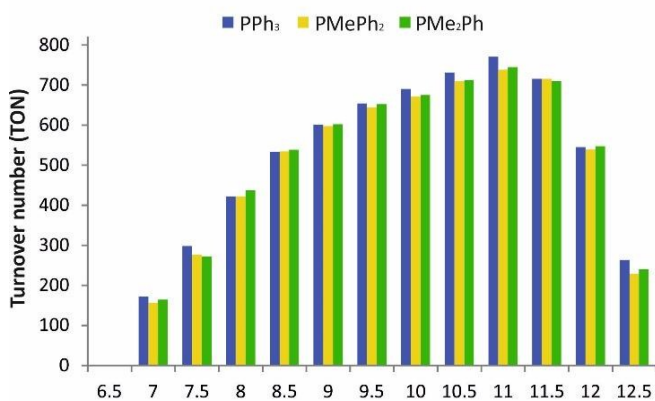


Figure 7: Hydrogen production at different pH-values with PPh₃ (blue), PMePh₂ (yellow) and PMe₂Ph (green); below 7.0 the system is inactive and the highest hydrogen production was achieved at a pH-value of 11.0; below 11.0 the reduction potential of the sacrificial donor is too low and above 11.0 the hydrogen concentration in the solution is reduced.

influence of different pH-values of the system different solutions with pH-values of 6.5 to 12.5 were adjusted by addition of HCl. Into these solutions 60 μmol/L of PS X, 90 μmol/L of Co-WRC and 180 μmol/L of either PPh₃, PMePh₂ or PMe₂Ph were added and the solutions were irradiated for 15 h. No hydrogen production was obvious under conditions at pH-values of 6.0 and 6.5. At a pH-value of 7.0 the hydrogen production was possible and the amount of produced hydrogen increased with higher pH-values up to a TON of 770 at pH 11. Above a pH-value of 11.5 the activity decreases strongly (see Figure 7). The exact hydrogen production data are illustrated in the ESI, chapter 5. A system including TEA as sacrificial donor can be influenced by two different antagonist effects. This behaviour is very well established in the literature.¹⁰ The first effect is the concentration of the proton (H⁺), if the pH-value is too high. However, the reduction potential of the sacrificial donor (TEA) is higher in basic condition.^{12,36,37} The proton concentration describes the accelerating of the reaction with higher concentration of protons in the solution. Based on the higher concentration the reduction is more likely. However the reduction property of the photosensitiser needs a higher pH-value for the activity and so the system is producing the most hydrogen at a pH-value of 11.

Influences of the phosphane ligands

To investigate the influence of phosphane ligands with different properties (Tolman cone angle, electron density) 7 phosphane ligands (180 μmol/L of PPh₃, PMePh₂, PMe₂Ph, P(4-An)₃ with An = Anisyl, P(2-An)₃, P(*n*Bu)₃ or P(*t*Bu)₃) were added to an irradiation solution with a pH-value of 11 with PS X (60 μmol/L) and Co-WRC (90 μmol/L) in a solution of ACN:TEA:H₂O

Table 3: Hydrogen production with phosphane ligands with different properties (electronic density and Tolman angle).

View Article Online

DOI: 10.1039/C6FD00210B

phosphane	TON	electronic-property	Tolman angle
PPh ₃	770	standard	145°
PMePh ₂	738	electron-rich	136°
PMe ₂ Ph	745	electron-rich	122°
P(4-An) ₃	733	electron-rich	148°
P(2-An) ₃	593	electron-rich	194°
P(<i>n</i> Bu) ₃	762	electron-poor	132°
P(<i>t</i> Bu) ₃	612	electron-poor	182°

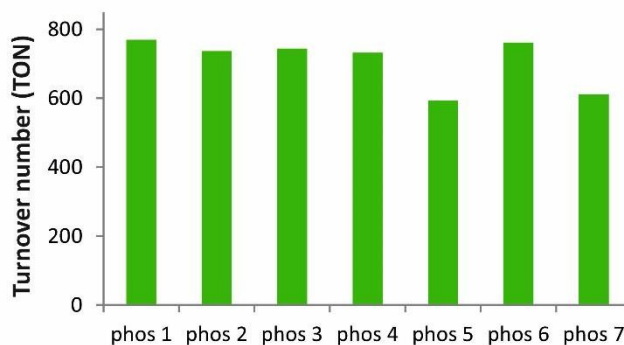


Figure 8: Hydrogen production with phosphane ligands with different properties; phosphane ligands with a big Tolman cone angle (>160°) cannot stabilise the Co(I) intermediate and the activity of the system decreases.

(4.5:4.5:1) and were irradiated for 12 h. This irradiation solution is equal to Entry 3 in Table 1. The phosphorus donor atoms of P(4-An)₃ and P(2-An)₃ are electron poorer than the phosphorus donor atom of PPh₃, however the phosphorus donor atoms of the other phosphane ligands PMePh₂, PMe₂Ph, P(*n*Bu)₃ and P(*t*Bu)₃ are electron richer. The chosen phosphane ligands have also different Tolman cone angles between 122° (PMe₂Ph) and 194° P(2-An)₃.³⁸ The obtained hydrogen production (turnover numbers) are shown in Figure 8 and in Table 3. The electronic density of the phosphane ligands has no major influence on the activity of the cobalt based water reduction catalysts. The turnover number with PPh₃ as the stock phosphane is 770. With a more electron rich ligand like P(*n*Bu)₃ the TON number based on the hydrogen production was 762 and with an electron poor phosphane ligand (P(4-An)₃) the turnover number of the produced hydrogen was 733. So these measurements are very similar and statistically equal. However, with phosphane ligands featuring a bigger Tolman angle the activity of the system is much lower (from 770 with PPh₃, Tolman cone angle = 145°, to 593 with P(2-An)₃, Tolman cone angle = 194°). The Tolman cone angle has a significant influence on the activity. Below a Tolman angle of 150° the interaction between the phosphane ligand and the Co(I) intermediate is quite strong and the Co(I) intermediate could be stabilised properly. If the Tolman angle is too big (>160°) the geometry of the system is distorted and so the intermediate cannot be stabilised enough and the stability of the hydrogen production system decreases and is in

the same range as the measurements without any addition of phosphane ligands.

Time resolved UV-Vis spectra

During the irradiation measurements the colour of the solution changed from yellowish to blue or green, depending on the system (with phosphane ligand, or without). To characterise the change of the colour and to understand the produced complexes in more detail UV-Vis spectra of selected photocatalytic systems were acquired during the irradiation process with a LED (365 nm). First Co-WRC (45 $\mu\text{mol/L}$) and PS X (30 $\mu\text{mol/L}$) were measured in a mixture of degassed ACN/ H_2O (1:1, v:v) without any addition of TEA as sacrificial donor. During the irradiation no changes of the UV/Vis spectrum were observed (plot A in Figure 9). Co-WRC is not reduced by PS X and so no photoinduced electron transfer happened. Without any sacrificial donor no Co(II) or Co(I) intermediate was produced and so no hydrogen could be generated. In the irradiation solution ACN: H_2O :TEA (4.5:4.5:1, v:v:v) with a pH-value of 11 the colour of the solution changed during the irradiation with the same LED (365 nm) and a peak with an absorption maximum at 487 nm (plot B in Figure 8) nm increased continuously. This absorption maximum is very well characteristic for Co(II) species,³⁶ which are produced by the reduction of the Co(III) based WRC by a one-electron step from the photosensitiser. In the presence of PPh_3 another peak with an absorption maximum at 643 nm increased, which is characteristic for Co(I) species (see plot C in Figure 9). First Co(II) is produced by the reduction of the Co(III) precatalyst and when all of the water reduction catalyst is reduced from Co(III) to Co(II) the second reduction step from Co(II) to Co(I) happened. The Co(II) intermediate is much more stable than the electron rich Co(I) intermediate without any stabilisation with a phosphane ligand in the irradiation solutions and so the Co(I) species just will be produced after the reduction of Co(III)-WRC to the Co(II) intermediate. PS X is able to reduce Co-WRC twice which is very important for the hydrogen production (two electron step), however the more important reduction step of Co(II) to Co(I) is not favoured without any addition of a phosphane ligand and this could be a reason of the lower hydrogen production.

During the irradiation with an addition of PPh_3 to stabilise the Co(I) species a completely different UV-Vis spectrum was observed. The absorption maxima at 487 nm were not detected, whereas another peak with an absorption maximum of 643 nm, which is based on Co(I)-phosphane complexes,¹⁰ was formed during the irradiation (see plot C in Figure 8). This spectrum is identical to the one obtained from dissolved single crystals of $[\text{Co}(\text{I})(\text{DO})(\text{DOH})\text{pn}(\text{PPh}_3)]$. This very important Co(I) species could be stabilised by PPh_3 as phosphane ligand. The reduction from Co(II) to Co(I) happens immediately after the reduction of Co(III) to Co(II). With these measurements a stabilising effect of PPh_3 is confirmed. It is also obvious that this detectable Co(I)-phosphane intermediate is very stable and so the time delayed hydrogen production can be explained. After an irradiation of 20 minutes the system without any phosphane addition was producing hydrogen with a TON of 103 and the system with an addition of PPh_3 was producing hydrogen after

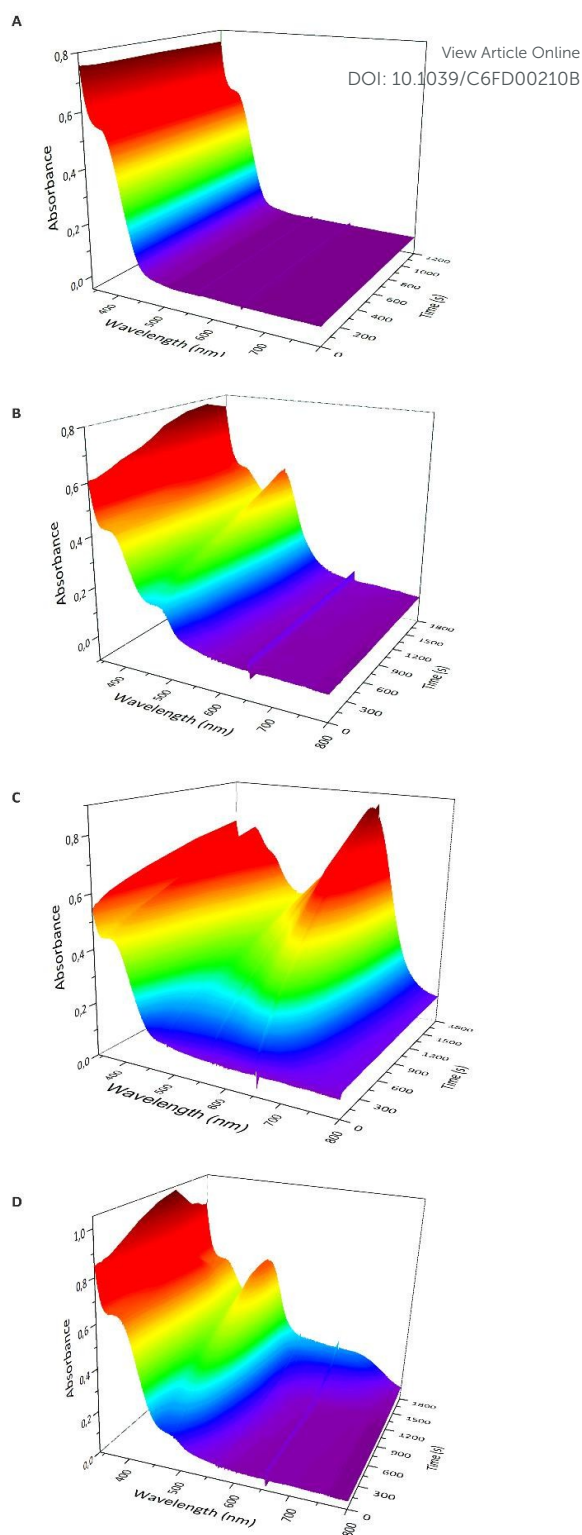


Figure 9: Time depending UV-Vis spectra during an irradiation with LED (365 nm); A = PS X and Co-WRC in ACN: H_2O ; B = PS X and Co-WRC in ACN: H_2O :TEA, C = with PPh_3 and D = with $\text{P}(\text{2-An})_3$.

the same time scale with a TON of 57. Phosphane ligands possessing a bigger bite angle than 160° showed a lower hydrogen production than with phosphane ligands with a

smaller bite angle. The different mechanisms are confirmed by time dependent UV-Vis measurements during an irradiation with an LED (365 nm). The UV-Vis spectra with an addition of P(2-An)₃ as phosphane ligand are completely different to the experiments with PPh₃ as phosphane ligand and are similar to the experiments without any phosphane ligand (see plot D in Figure 9). Therefore these results can be explained by non-stabilisation of the Co(I) intermediate by a typical sterically hindered phosphane ligand.

Electrochemical measurements

The addition of PPh₃ to a solution of Co-WRC in acetonitrile and TBAPF₆ (0.1 mol/L) has no effect on the reduction of the Co(III) centre to the Co(II) centre. The first reduction step has a similar value of -0.641 eV with an addition of PPh₃ to -0.643 eV without

Quenching process

The influences of the quenching of PS X were analysed with the water reduction catalyst (Co-WRC) in different solutions: a) Co-WRC in ACN:H₂O (v:v =1:1); b) Co-WRC in ACN:TEA (v:v = 9:1); c) Co-WRC in ACN:H₂O:TEA (v:v:v =4.5:4.5:1); d) in the solution of c with the addition of 2 eq. of PPh₃. All the quenching processes have been studied by steady-state fluorescence spectroscopy and the excited state lifetimes were performed with time resolved methods. The emission spectra of all measurements are illustrated in the ESI, pages 12 and 13.

First the influence of Co-WRC in ACN was detected. The

eq. of Co-WRC	ACN		ACN/TEA (9:1)		irr. solution		irr. sol. + 2 eq. PPh ₃	
	I ₀ /I	τ ₀ /τ	I ₀ /I	τ ₀ /τ	I ₀ /I	τ ₀ /τ	I ₀ /I	τ ₀ /τ
0	1.000	1.000	1.000	1.000	1.000	1.000	1.000	1.000
1	1.354	1.312	1.313	1.298	1.179	1.165	1.246	1.232
2	1.812	1.654	1.745	1.659	1.382	1.368	1.564	1.514
4	2.432	2.398	2.296	2.215	1.604	1.521	1.950	1.868
8	3.547	3.354	3.345	3.165	2.339	2.254	2.842	2.710
20	5.875	5.825	5.598	5.498	3.874	3.649	4.736	4.574

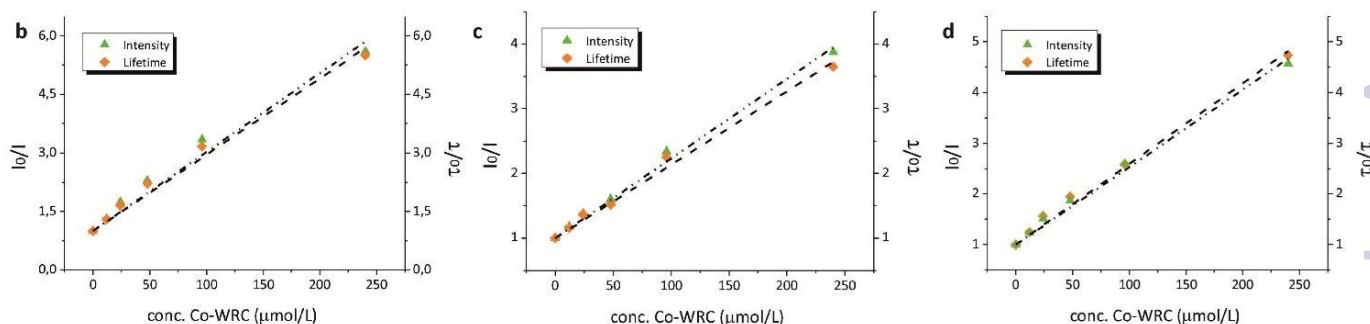
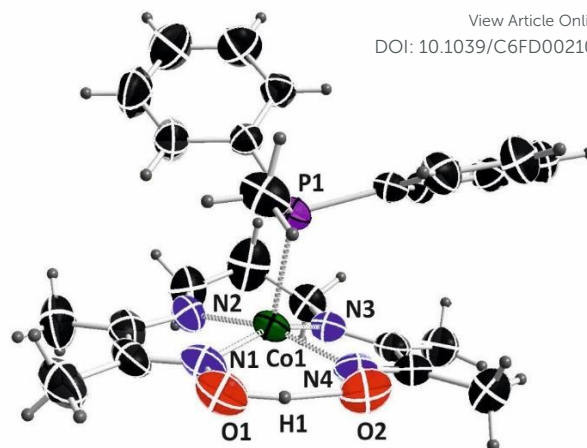


Figure 10: Table: photophysical measurements with different concentrations of Co-WRC in a solution of PS X ($c = 5 \mu\text{mol/L}$) in different solutions (a = ACN; b = ACN/TEA; c = irradiation solution; d = irradiation solution + 2 eq. of PPh₃); Graphs: Stern Volmer plots of the quenching mechanism; green triangles = quenching of the emission intensity and orange diamonds represent the quenching of the excited state lifetimes, the excited state lifetimes were measured during time resolved measurements, whereas the emission spectra of all measurements are illustrated in the ESI, pages 12 and 13.

any addition of PPh₃.¹⁰ The second reduction from Co(II) to Co(I) is influenced by PPh₃. The reduction peak of Co(II) to Co(I) is shifted to lower negative potential, so the phosphane can stabilise the Co(I) intermediate of the catalytic pathway. The reduction peak of Co(II)/Co(I) is shifted from -1.141 V to -0.825 V at a scanning rate of 0.1 V/s.¹⁰ The CV measurements with an addition of P(2-An)₃ as phosphane ligand showed similar CV spectra compared to the Co-WRC alone. The phosphane ligand with a very huge bite angle of 194° could not stabilise the second reduction step and so the CV spectrum looks like the CV spectrum without any addition of a phosphane ligand. For comparison of the major effect of PPh₃ to the second reduction step, the three different CV-measurements are illustrated in the ESI, Figure 9.

quenching mechanism followed a dynamic quenching mechanism. The quenching of the emission with a Stern Volmer constant of $21060 \pm 26 \text{ L} \cdot \text{mol}^{-1}$ ($R^2 = 0,9901$) and a dynamic quenching constant of $6.1 \cdot 10^{10} \text{ L} \cdot \text{mol}^{-1} \cdot \text{s}^{-1}$ is quite high. For a quenching mechanism including singlet excited state complexes with short excited state lifetimes ($\sim 1\text{ns}$) the dynamic quenching constant would be too high and a quenching efficiency of more than 1.0 would be determined.³⁹ For triplet excited state complexes with a excited state lifetime of more than 100 ns (PS X, $\tau = 346 \text{ ns}$) the dynamic quenching constant is much higher than for singlet excited state complexes based on the directly proportional relation of the Stern Volmer constant to the excited state lifetime ($k_q \cdot \tau^0 = k_{sv}$). The efficiency of this quenching process has a value of 0.24. A sufficient quenching behaviour is very important for a successful reaction (photocatalytic hydrogen production). The Stern Volmer plots

of the excited state lifetimes (orange diamonds) and the emission maxima (green triangles) are shown in Figure 10 plot a. The Stern Volmer constant with $20023 \pm 24 \text{ L} \cdot \text{mol}^{-1}$ ($R^2 = 0.9884$) and the dynamic quenching constant of $5.8 \cdot 10^{10} \text{ L} \cdot \text{mol}^{-1} \cdot \text{s}^{-1}$ in a mixture of ACN:TEA (v:v = 9:1) show quite similar values like the experiments without any TEA. There is no influence of TEA to the quenching mechanism, which is very useful for a good reaction. The Stern Volmer plot is illustrated in Figure 10 plot b. The Stern Volmer constant in the irradiation solution (ACN:H₂O:TEA; v:v:v = 4.5:4.5:1) is with $11340 \pm 56 \text{ L} \cdot \text{mol}^{-1}$ ($R^2 = 0.9873$) less than without any water. The quenching constant is $3.3 \cdot 10^{10} \text{ L} \cdot \text{mol}^{-1} \cdot \text{s}^{-1}$ and so the water has an effect on the quenching mechanism of the system (see Table in Figure 10). The water reduction catalyst has different UV-Vis spectra in the different solvents like H₂O, TEA and ACN. The change of the properties of the solution changes the solution sphere of the water reduction catalyst and so the water reduction catalyst is slightly protected from a collision with the photosensitiser. However the system will be quenched and so an energy transfer occurs and it is also possible to transfer an electron from PS X to Co-WRC. The quenching during the experiments with an addition of PPh₃ is slightly higher than without PPh₃ ($4.5 \cdot 10^{10} \text{ L} \cdot \text{mol}^{-1} \cdot \text{s}^{-1}$ for the dynamic quenching constant and $15832 \pm 61 \text{ L} \cdot \text{mol}^{-1}$ ($R^2 = 0.9891$) for the Stern Volmer constant). Two possibilities could happen. First PPh₃ coordinates to the water reduction catalyst and the produced adduct of the two components quenches the photosensitiser in a different way. Or PPh₃ quenches the photosensitiser as well. The second way should be preferred, because the Co(III) complex has no affinity to the phosphane as ligand. The phosphane will interact just with Co(I) and maybe slightly with Co(II), however a reduction of the water reduction catalyst during the short time measurement can be excluded. It is not alarming that the photosensitiser is also quenched by PPh₃. During the irradiation the phosphane stabilises the reduced form of Co-WRC and so the photosensitiser will not be quenched by the phosphane in this high amount. The produced hydrogen confirms the activity of this system. This could explain the fact that the initial rate of hydrogen production is larger without any phosphane during the first two hours (see Fig. 6). Only then the stabilisation effect of the phosphane becomes beneficial. Maybe this is also responsible for the time-delayed hydrogen production in the first few minutes.



View Article Online
DOI: 10.1039/C6FD00210B

Figure 11: ORTEP plot of $[\text{Co}(\text{I})(\text{DO})(\text{DOH})\text{pn}(\text{PMePh}_2)]$, important bond lengths (Å) and bond angles (°) are shown; Co1-P1 = 2.2113(9) Å, Co1-N1 = 1.863(3) Å, Co1-N2 = 1.883(3) Å, Co1-N3 = 1.888(3) Å, Co1-N4 = 1.856(3) Å, N1-O1 = 1.361(3) Å, N4-O2 = 1.361(3) Å, O1-H1 = 1.04(3) Å, O2-H1 = 1.42(3) Å, N1-Co1-N2 = 80.97(12)°, N2-Co1-N3 = 96.48(11)°, N3-Co1-N4 = 80.95(12)°, N4-Co1-N1 = 95.50(12)°, N1-Co1-P1 = 98.24(8)°, N2-Co1-P1 = 103.80(8)°, N3-Co1-P1 = 102.36(8)°, N4-Co1-P1 = 93.00(8)°.

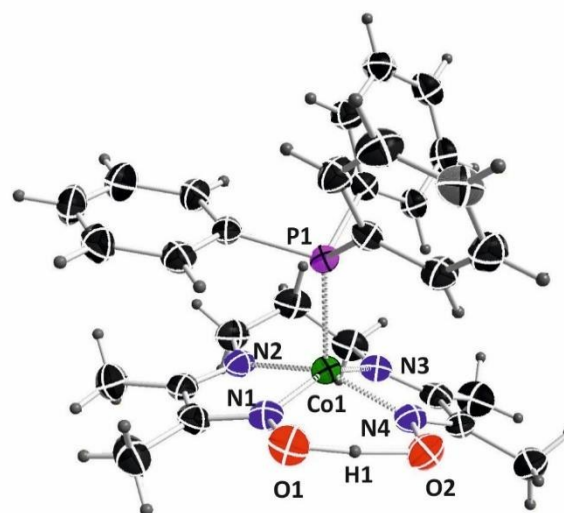


Figure 12: ORTEP plot of $[\text{Co}(\text{I})(\text{DO})(\text{DOH})\text{pn}(\text{PPh}_3)]$, important bond lengths (Å) and bond angles (°) are shown; Co1-P1 = 2.2514(11) Å, Co1-N1 = 1.864(2) Å, Co1-N2 = 1.901(2) Å, Co1-N3 = 1.899(2) Å, Co1-N4 = 1.869(2) Å, N1-O1 = 1.358(3) Å, N4-O2 = 1.364(3) Å, O1-H1 = 1.12(3) Å, O2-H1 = 1.33(3) Å, N1-Co1-N2 = 80.89(10)°, N2-Co1-N3 = 94.36(10)°, N3-Co1-N4 = 80.64(10)°, N4-Co1-N1 = 92.83(10)°, N1-Co1-P1 = 95.12(8)°, N2-Co1-P1 = 96.75(7)°, N3-Co1-P1 = 110.74(7)°, N4-Co1-P1 = 108.18(7)°.

Investigation of the Co(I) intermediate

The catalytic mechanism of $[\text{Co}(\text{III})(\text{DO})(\text{DOH})\text{pnBr}_2]$ is already discussed in the literature with $[\text{Ir}(\text{ppy})(\text{bpy})]^+$ as

photosensitiser.⁴⁰ [Cu(Xantphos)(Bathocuproine)](PF₆) as photosensitiser has quite similar properties to [Ir(ppy)(bpy)]⁺ and so the reductive quenching of the photosensitiser followed by the reduction of [Co(III)(DO)(DOH)pnBr₂] to a Co(I)-intermediate seems to show most likely the same mechanism. However it was not possible to characterise completely the Co(I) intermediate, before. This photogenerated Co(I) intermediate is the catalytically active species of a Co(III) precatalyst^{10,29,41–43} which was characterised for the first time by X-ray crystallography in our working group. The Co(III) catalyst was reduced in the presence of NaBH₄ and is stabilised by different phosphane ligands and after crystallisation of these complexes it was possible to determine two molecular structures of [Co(I)(DO)(DOH)pn(phos)] with PPh₃ and PMePh₂ as phosphane ligands with X-ray measurements, which are illustrated in Figures 11 and 12. A similar molecular structure via X-ray measurement of [Co(I){C2(DO)(DOH)pn}(PPh₃)] was obtained by G. Finke and co-workers,⁴⁴ but has not been catalytically tested. The difference between these structures are the substitutions of the oxime-backbone. [Co(I){C2(DO)(DOH)pn}(PPh₃)] has a mixed substitution with one methyl and one ethyl group, whereas [Co(I)(DO)(DOH)pn(phos)] just shows methyl groups. The bond lengths between Co(I) as metal centre and the phosphorus atom of the phosphane ligand are 2.2514(11) Å for PPh₃ as phosphane ligand and 2.1113(9) Å for PMePh₂, which are characteristic for a coordination bond between a phosphane ligand and a Co(I) metal centre. All the other bond lengths and bond angles are shown in the ESI, chapter 8 and the figure legends of Figures 11 and 12. This Co(I) intermediate is stabilised by the phosphane ligands and is able to react with two protons to reduce them during the catalytic cycle.

Theoretical calculations

The theoretical calculations were performed under vacuum conditions with the Functional PBE1PBE and with the Basic sets TZVP for the Co metal centre and 6-31G(d,p) for the other elements (C, H, N, O, P) and the time resolved UV-Vis spectrum calculation was performed in an ACN sphere. The bond lengths

Table 4: Hydrogen production with phosphane ligands with different properties (electronic density and Tolman cone angle) compared to the bond lengths between the Co(I) centres and the phosphane ligands; with a bond length below 2.3 Å the Co(I) intermediate was stabilised and the hydrogen production was higher; with a bond length above 2.5 Å, it was lower based on non-stabilisation effects of the Co(I) intermediate.

Compound	Co-P-length (Å)	Tolman angle (°)	electron-density	TON
Co-PPh ₃	2.2433	145	standard	770
Co-PMePh ₂	2.1983	136	rich	738
Co-PMe ₂ Ph	2.1793	122	rich	745
Co-PMe ₃	2.1776	118	rich	--
Co-P(4-An) ₃	2.2829	148	poor	733
Co-P(2-An) ₃	2.5866	194	poor	593
Co-P <i>n</i> Bu ₃	2.2102	132	rich	762
Co-P <i>t</i> Bu ₃	2.5482	182	rich	612

and the bond angles of the theoretical calculation were compared with the obtained molecular structure of the X-ray measurements. All the bond lengths and bond angles are shown in the ESI, chapter 9. In order to gain further insights into the electronic transitions, time dependent DFT calculations were carried out applying the same functional as well as basic sets. The calculated and measured UV-Vis spectra of [Co(DO)(DOH)pnPPh₃], obtained by a reduction of Co(III)-WRC in the presence of PPh₃ to Co(I)-WRC are displayed in Figure 10, ESI. Spectra are coinciding with each other. The calculated UV-Vis bands and the measured UV-Vis spectrum are in good agreement with the experimental data and therefore the theoretical calculation can explain the interactions of Co(I) in a proper way. The UV-Vis absorption bands of the time dependent UV-Vis measurements can also be explained with these calculations. The most important information of the calculated structures is the bond length between the cobalt metal centre and the phosphorus atom of the different phosphane ligands (PPh₃, PMePh₂, PMe₂Ph, P(4-An)₃, P(2-An)₃, P(*n*Bu)₃, P(*t*Bu)₃). These calculated bond lengths compared with the Tolman cone angles, the electron density and the produced hydrogen with PS X as photosensitiser are shown in Table 4. The theoretical calculations are fitting perfectly because the bond length between Co(I) and PPh₃ was 2.2514(11) Å for the X-ray measurement and 2.2433 Å for the theoretical calculation. The same result was obtained with PMePh₂ with 2.2113(9) Å for the X-ray measurement and 2.1983 Å with the theoretical calculation. The results of the theoretical calculations with PPh₃ are illustrated in the ESI, Table 13. During the sunlight induced hydrogen production with an addition of a phosphane ligand with a Tolman cone angle below 160° (PPh₃ = 770, PMePh₂ = 738, PMe₂Ph = 745, P(4-An)₃ = 733, P(*n*Bu)₃ = 762) a higher hydrogen production was obtained (see Table 4). With the two other phosphane ligands with a Tolman cone angle above 160° (P(2-An)₃ = 593 and P(*t*Bu)₃ = 612) the hydrogen production was significantly lower and in the same range as without any addition of phosphane (with pH = 11, TON = 578). In agreement with the photocatalytic measurements phosphane ligands, that interact with the Co(I) metal centres, stabilise the Co(I) intermediate and increased the TON. The theoretical calculation predicts, that all phosphane ligands except P(2-An)₃ and P(*t*Bu)₃ connect with a Co(I) metal centre *via* a coordinative way (bond lengths between 2.17 Å and 2.28 Å, see Table 4). For every phosphane ligand which interacted with the Co(I) metal centre, the Co(I) intermediates were stabilised and the TON increased, where the photocatalytic measurements confirm this assumption. With a calculated bond length between 2.50 Å and 2.60 Å no stabilization of the Co(I) intermediate was obvious and the hydrogen production was lower.

Conclusions

Intramolecular approach

We have shown that [Os(bpy)₂(dppcb)Pd(dppm)](PF₆)₄ is one of the most stable dyad systems for sunlight induced hydrogen production in an intramolecular way due to the phosphane

stabilisation by dppcb and dppm. This complex is stable for 1412 h and is able to produce hydrogen up to a turnover number of 267. The photoinduced electron transfer was analysed with photophysical and electrochemical measurements of the dyad system as well as of the homometallic complexes $[\text{Os}(\text{bpy})_2(\text{dppcb})\text{Os}(\text{bpy})_2](\text{PF}_6)_4$, $[\text{Pd}(\text{dppm})(\text{dppcb})\text{Pd}(\text{dppm})](\text{PF}_6)_4$ and $[\text{Os}(\text{bpy})_2(\text{cis-dppen})](\text{PF}_6)_2$. Furthermore the molecular structure was analysed with X-ray measurements.

Intermolecular approach

All the analytic methods used (UV-Vis spectroscopy during irradiation, CV measurements and theoretical calculations) show the importance of a phosphane ligand to stabilise the Co(I) intermediate during a photochemical pathway. The phosphane ligands PPh_3 , PMePh_2 , PMe_2Ph , $\text{P}(4\text{-An})_3$, and $\text{P}(n\text{Bu})_3$ are able to stabilise the Co(I) intermediate and therefore the activity of the system containing these phosphane ligands is higher than with the two monophosphane ligands with a huge Tolman angle $\text{P}(2\text{-An})_3$ and $\text{P}(t\text{Bu})_3$. The required space of these two ligands is too big and so the phosphane ligands could not interact with a Co(I) intermediate. With $\text{P}(2\text{-An})_3$ a completely different UV-Vis spectrum during the irradiation compared to PPh_3 was observed. In the presence of $\text{P}(2\text{-An})_3$ and without any addition of a phosphane ligand a UV-Vis peak around 487 nm was detected, which is based on a Co(II)-H intermediate. This complex was theoretically investigated by Fujita and Muckerman.⁴⁵ The Co(II) intermediate of the catalytic pathway was also reported during light induced hydrogen production,^{10,46} during electrochemical studies⁴⁷, and it was identified in electrochemical reactions.^{42,43} During light irradiated UV-Vis measurements of the system containing PPh_3 a band, which is representing a Co(II)-H was not detectable. The Co-WRC was reduced directly to Co(I) and was stabilised producing Co(I)- PPh_3 , which absorbs at 643 nm. This UV-Vis spectrum was also calculated by means of TD-DFT in this work. It is also identical to the spectrum obtained from the dissolved single crystals used for X-ray diffraction shown in Fig. 12 for the first time. With the help of theoretical calculations the coherence between the bite angle of monophosphane ligands and the bond lengths between these monophosphane ligands and the Co(I) intermediate of Co-WRC was analysed and the experimental measurements were confirmed. Though the catalytic mechanism, homolytic or heterolytic, cannot be distinguished by the theoretical calculations, they clearly confirm the Co(I) stabilization by phosphine coordination. The stabilisation of a Co(I) intermediate of Co-WRC has a major influence on the activity of the system. The coordinated phosphane ligand should have a smaller Tolman angle than 160° . Finally, it is important to note that the photocatalytically active species completely characterised for the first time in this work by single crystal X-ray structure analysis correspond to the species obtained under LED light (compare Figure 9), since they show identical UV-Vis spectra (compare Figure 10, ESI).¹⁰

Acknowledgements

This research was financially supported by the Austrian Research Promotion Agency (FFG, project numbers 834430 and 841186), Vienna, Austria, the Climate and Energy Fund of the Austrian government, the companies VERBUND AG and D. Swarovski KG, and by the Austrian Agency for International Cooperation in Education and Research (OEAW).

References

- 1 J. Kim, C. A. Henao, T. A. Johnson, D. E. Dedrick, J. E. Miller, E. B. Stechel and C. T. Maravelias, *Energy Environ. Sci.*, 2011, **4**, 3122.
- 2 N. Armaroli and V. Balzani, *ChemSusChem*, 2011, **4**, 21–36.
- 3 J. H. Alstrum-Acevedo, M. K. Brennaman and T. J. Meyer, *Inorg. Chem.*, 2005, **44**, 6802–6827.
- 4 K. Maeda, *ACS Catal.*, 2013, **3**, 1486–1503.
- 5 S. Rau, B. Schäfer, D. Gleich, E. Anders, M. Rudolph, M. Friedrich, H. Görls, W. Henry and J. G. Vos, *Angew. Chem. Int. Ed. Engl.*, 2006, **45**, 6215–6218.
- 6 M. Schulz, J. Hirschmann, A. Draksharapu, G. Singh Bindra, S. Soman, A. Paul, R. Groarke, M. T. Pryce, S. Rau, W. R. Browne and J. G. Vos, *Dalton Trans.*, 2011, **40**, 10545–10552.
- 7 S. M. Arachchige, J. Brown and K. J. Brewer, *Journal of Photochemistry and Photobiology A: Chemistry*, 2008, **197**, 13–17.
- 8 A. Fihri, V. Artero, A. Pereira and M. Fontecave, *Dalton Trans.*, 2008, 5567–5569.
- 9 J. Prock, C. Strabler, W. Viertl, H. Kopacka, D. Obendorf, T. Müller, E. Tordin, S. Salz, G. Knör, M. Mauro, L. de Cola and P. Brüggeller, *Dalton Trans.*, 2015.
- 10 P. Zhang, P.-A. Jacques, M. Chavarot-Kerlidou, M. Wang, L. Sun, M. Fontecave and V. Artero, *Inorg. Chem.*, 2012, **51**, 2115–2120.
- 11 a) F. Gärtner, B. Sundararaju, A.-E. Surkus, A. Boddien, B. Loges, H. Junge, P. H. Dixneuf and M. Beller, *Angew. Chem. Int. Ed. Engl.*, 2009, **48**, 9962–9965; b) F. Gärtner, D. Cozzula, S. Losse, A. Boddien, G. Anilkumar, H. Junge, T. Schulz, N. Marquet, A. Spannenberg, S. Gladiali and M. Beller, *Chemistry*, 2011, **17**, 6998–7006; c) D. R. Whang, K. Sakai and S. Y. Park, *Angew. Chem. Int. Ed.*, 2013, **52**, 11612–11615;
- 12 J. Hawecker, J. M. Lehn, R. Ziessel, *Nouv. J. Chim.*, **1983**, 271–277.
- 13 a) W. R. McNamara, Z. Han, P. J. Alperin, W. W. Brennessel, P. L. Holland and R. Eisenberg, *J. Am. Chem. Soc.*, 2011, **133**, 15368–15371; b) D. Streich, Y. Astuti, M. Orlandi, L. Schwartz, R. Lomoth, L. Hammarström and S. Ott, *Chemistry*, 2010, **16**, 60–63;
- 14 M. P. McLaughlin, T. M. McCormick, R. Eisenberg and P. L. Holland, *Chem. Commun. (Camb.)*, 2011, **47**, 7989–7991.
- 15 Y. Na, M. Wang, J. Pan, P. Zhang, B. Åkermark and L. Sun, *Inorg. Chem.*, 2008, **47**, 2805–2810.
- 16 T. M. McCormick, B. D. Calitree, A. Orchard, N. D. Kraut, F. V. Bright, M. R. Detty and R. Eisenberg, *J. Am. Chem. Soc.*, 2010, **132**, 15480–15483.

- 17 Z. Han, W. R. McNamara, M.-S. Eum, P. L. Holland and R. Eisenberg, *Angew. Chem. Int. Ed.*, 2012, **51**, 1667–1670.
- 18 K. Kalyanasundaram and D. Dung, *J. Phys. Chem.*, 1980, **84**, 2551–2556.
- 19 a) P. Poddutoori, D. T. Co, A. P. S. Samuel, C. H. Kim, M. T. Vagnini and M. R. Wasielewski, *Energy Environ. Sci.*, 2011, **4**, 2441; b) H. Yamaguchi, T. Onji, H. Ohara, N. Ikeda and A. Harada, *Bull. Chem. Soc. Jpn.*, 2009, **82**, 1341–1346;
- 20 a) R. S. Khnayzer, C. E. McCusker, B. S. Olaiya and F. N. Castellano, *J. Am. Chem. Soc.*, 2013, **135**, 14068–14070; b) C. E. McCusker and F. N. Castellano, *Inorg. Chem.*, 2013, **52**, 8114–8120;
- 21 M. Karnahl, E. Mejía, N. Rockstroh, S. Tschierlei, S.-P. Luo, K. Grabow, A. Kruth, V. Brüser, H. Junge, S. Lochbrunner and M. Beller, *ChemCatChem*, 2014, **6**, 82–86.
- 22 E. Mejía, S.-P. Luo, M. Karnahl, A. Friedrich, S. Tschierlei, A.-E. Surkus, H. Junge, S. Gladiali, S. Lochbrunner and M. Beller, *Chemistry*, 2013, **19**, 15972–15978.
- 23 S.-P. Luo, E. Mejía, A. Friedrich, A. Pazidis, H. Junge, A.-E. Surkus, R. Jackstell, S. Denurra, S. Gladiali, S. Lochbrunner and M. Beller, *Angew. Chem. Int. Ed. Engl.*, 2013, **52**, 419–423.
- 24 a) N. Armaroli, G. Accorsi, M. Holler, O. Moudam, J.-F. Nierengarten, Z. Zhou, R. T. Wegh and R. Welter, *Adv. Mater.*, 2006, **18**, 1313–1316; b) C. Bizzarri, C. Strabler, J. Prock, B. Trettenbrein, M. Ruggenthaler, C.-H. Yang, F. Polo, A. Iordache, P. Brüggegger and L. de Cola, *Inorg. Chem.*, 2014, **53**, 10944–10951; c) R. D. Costa, D. Tordera, E. Ortí, H. J. Bolink, J. Schönle, S. Graber, C. E. Housecroft, E. C. Constable and J. A. Zampese, *J. Mater. Chem.*, 2011, **21**, 16108; d) L. He, L. Duan, J. Qiao, D. Zhang, L. Wang and Y. Qiu, *Chem. Commun. (Camb.)*, 2011, **47**, 6467–6469; e) Q. Zhang, Q. Zhou, Y. Cheng, L. Wang, D. Ma, X. Jing and F. Wang, *Adv. Funct. Mater.*, 2006, **16**, 1203–1208;
- 25 a) T. McCormick, W.-L. Jia and S. Wang, *Inorg. Chem.*, 2006, **45**, 147–155; b) Q. Zhang, J. Ding, Y. Cheng, L. Wang, Z. Xie, X. Jing and F. Wang, *Adv. Funct. Mater.*, 2007, **17**, 2983–2990; c) J. Min, Q. Zhang, W. Sun, Y. Cheng and L. Wang, *Dalton Trans.*, 2011, **40**, 686–693; d) C. Femoni, S. Muzzioli, A. Palazzi, S. Stagni, S. Zacchini, F. Monti, G. Accorsi, M. Bolognesi, N. Armaroli, M. Massi, G. Valenti and M. Marcaccio, *Dalton Trans.*, 2013, **42**, 997–1010; e) R. Hou, T.-H. Huang, X.-J. Wang, X.-F. Jiang, Q.-L. Ni, L.-C. Gui, Y.-J. Fan and Y.-L. Tan, *Dalton Trans.*, 2011, **40**, 7551–7558;
- 26 a) M. Wang, L. Chen, X. Li and L. Sun, *Dalton Trans.*, 2011, **40**, 12793–12800; b) N. Wang, M. Wang, L. Chen and L. Sun, *Dalton Trans.*, 2013, **42**, 12059–12071; c) N. Wang, M. Wang, Y. Wang, D. Zheng, H. Han, M. S. G. Ahlquist and L. Sun, *J. Am. Chem. Soc.*, 2013, **135**, 13688–13691; d) W. Gao, J. Sun, T. Åkermark, M. Li, L. Eriksson, L. Sun and B. Åkermark, *Chemistry*, 2010, **16**, 2537–2546;
- 27 a) M. A. Gross, A. Reynal, J. R. Durrant and E. Reisner, *J. Am. Chem. Soc.*, 2014, **136**, 356–366; b) P. Du, J. Schneider, P. Jarosz, J. Zhang, W. W. Brennessel and R. Eisenberg, *J. Phys. Chem. B*, 2007, **111**, 6887–6894; c) A. Das, Z. Han, W. W. Brennessel, P. L. Holland and R. Eisenberg, *ACS Catal.*, 2015, **5**, 1397–1406;
- 28 a) V. Artero, M. Chavarot-Kerlidou and M. Fontecave, *Angew. Chem. Int. Ed.*, 2011, **50**, 7238–7266; b) W. T. Eckenhoff, W. R. McNamara, P. Du and R. Eisenberg, *Biochimica et Biophysica Acta (BBA) - Bioenergetics*, 2013, **1827**, 958–973;
- 29 P.-A. Jacques, V. Artero, J. Pécaut and M. Fontecave, *Proc. Natl. Acad. Sci. U S A*, 2009, **106**, 20627–20632.
- 30 W. Oberhauser, C. Bachmann, T. Stampfl, R. Haid, C. Langes, H. Kopacka, A. Rieder and P. Brüggegger, *Inorganica Chimica Acta*, 1999, **290**, 167–179.
- 31 R. Gutmann, S. Eller, M. Fessler, W. E. van der Veer, A. Dumfort, H. Kopacka, T. Müller and P. Brüggegger, *Inorganic Chemistry Communications*, 2007, **10**, 1510–1514.
- 32 T. Yang, A. Xia, Q. Liu, M. Shi, H. Wu, L. Xiong, C. Huang and F. Li, *J. Mater. Chem.*, 2011, **21**, 5360–5367.
- 33 A. Fihri, V. Artero, M. Razavet, C. Baffert, W. Leibl and M. Fontecave, *Angew. Chem.*, 2008, **120**, 574–577.
- 34 C. M. Strabler, J. Prock, W. Viertl, R. Pehn, A. Weninger, H. Kopacka, D. Obendorf and P. Brüggegger, *Materials Today: Proceedings*, 2016, **3**, 183–187.
- 35 S. Fischer, D. Hollmann, S. Tschierlei, M. Karnahl, N. Rockstroh, E. Barsch, P. Schwarzbach, S.-P. Luo, H. Junge, M. Beller, S. Lochbrunner, R. Ludwig and A. Brückner, *ACS Catal.*, 2014, **4**, 1845–1849.
- 36 P. Du, K. Knowles and R. Eisenberg, *J. Am. Chem. Soc.*, 2008, **130**, 12576–12577.
- 37 a) B. Probst, A. Rodenberg, M. Guttentag, P. Hamm and R. Alberto, *Inorg. Chem.*, 2010, **49**, 6453–6460; b) P. Zhang, M. Wang, J. Dong, X. Li, F. Wang, L. Wu and L. Sun, *J. Phys. Chem. C*, 2010, **114**, 15868–15874;
- 38 a) C. A. Tolman, *J. Am. Chem. Soc.*, 1970, **92**, 2956–2965; b) C. A. Tolman, *Chem. Rev.*, 1977, **77**, 313–348; c) W. E. Steinmetz, *Quant. Struct.-Act. Relat.*, 1996, **15**, 1–6.
- 39 V. Balzani, A. Juris and P. Ceroni, *Photochemistry and photophysics. Concepts, research, applications*, Wiley-VCH, Weinheim, 2014.
- 40 N. Kaeffer, M. Chavarot-Kerlidou and V. Artero, *Acc. Chem. Res.*, 2015, **48**, 1286–1295.
- 41 C. Baffert, V. Artero and M. Fontecave, *Inorg. Chem.*, 2007, **46**, 1817–1824.
- 42 J. L. Dempsey, J. R. Winkler and H. B. Gray, *J. Am. Chem. Soc.*, 2010, **132**, 16774–16776.
- 43 X. Hu, B. S. Brunschwig and J. C. Peters, *J. Am. Chem. Soc.*, 2007, **129**, 8988–8998.
- 44 T. J. R. Weakley, J. Marks and R. G. Finke, *Acta Crystallogr. C Cryst. Struct. Commun.*, 1994, **50**, 1690–1692.
- 45 J. T. Muckerman and E. Fujita, *Chem. Commun.*, 2011, **47**, 12456.
- 46 P. Du, J. Schneider, G. Luo, W. W. Brennessel and R. Eisenberg, *Inorg. Chem.*, 2009, **48**, 4952–4962.
- 47 O. Pantani, E. Anxolabéhère-Mallart, A. Aukauloo and P. Millet, *Electrochemistry Communications*, 2007, **9**, 54–58.